Journal of Visualization, Vol. 10, No. 3 (2007)289-298

Regular Paper

Pressure-Sensitive Paint Measurement of the Flow around a Simplified Car Model

Yamashita, T.*[1], Sugiura, H.*[1], Nagai, H.*[1], Asai, K.*[1] and Ishida, K.*[2]

*1 Department of Aerospace Engineering, Tohoku University, Sendai, Miyagi, 980-8579, Japan.
*2 NISSAN Motor Co. Ltd., Atsugi, Kanagawa, 243-0192, Japan.

Received 16 October 2006
Revised 15 May 2007

Abstract : In applying Pressure-Sensitive Paint (PSP) to low-speed flow wind tunnel testing, it is important to minimize any measurement uncertainties. There are various error sources such as camera noise, misalignment of images due to model displacement and temperature distribution over the model. Among these factors, the effects of temperature distribution change during tests on pressure measurement accuracies were studied in the present paper. Pressure and temperature distributions over a simplified car model (1/10 scale Ahmed model) were measured using PSP and Temperature-Sensitive Paint (TSP). Sequential images were acquired at the same intervals over the entire test period, including for the conditions before and after the tunnel run. As a result, it was found that the measurement error caused by temperature distribution over the model could be reduced using a single-point temperature measurement. In addition, by measuring surface temperature distributions on the model using TSP, it was proved that the most accurate pressure measurement could be made by rationing the wind-off image acquired immediately after shutting down the tunnel to the wind-on image acquired immediately before shutting down the tunnel. Using the present measurement technique, complicated pressure fields over the Ahmed model were successfully visualized.

Keywords : Pressure-Sensitive Paint (PSP), Low-speed wind tunnel, Ahmed model, Oil flow.

1. Introduction

Recently Pressure-Sensitive Paint (PSP) has been applied to various research fields (Bell et al., 2001). In recent years, the automobile industries have become aware of this new technique and expect to use PSP as a working tool for aerodynamic design and for validating CFD codes. However it is difficult to apply PSP to low-speed flow regions, because the pressure changes around a model in low-speed flow are very small. For example, in the case of the freestream velocity $U = 50$ m/s, the dynamic pressure is as small as 1.5 kPa, which is comparable to the measurement accuracy of current PSP techniques.

To resolve such slight pressure changes, it is necessary to minimize various measurement errors, such as optical noise, model displacement and deformation, temperature distribution over the model and so on (Sant et al., 2001; Engler et al., 2002; Mebarki et al., 2002). Optical noise, i.e., shot-noise of CCD camera, can be reduced by ensemble averaging, and the effects of model displacement and deformation can be corrected by image registration techniques. Thus, the dominant remaining error source is that of errors caused by temperature distribution over a model. In a closed-circuit wind tunnel, the flow temperature usually changes with time, causing a change in model surface temperature during a test. Brown (2000), Bell (2004) and Mitsuo et al. (2005) showed

that errors due to temperature change can be minimized when the model was placed in a flow for an extended period to enable an equilibrium state in the model surface temperature and the wind-off image was then acquired immediately after stopping the tunnel is shut down. However, it is not certain whether this approach would be effective over the entire model surface, since an in-situ calibration method was used in the previous studies.

In the present research, a simplified car model known as the Ahmed model was tested in a low-speed wind tunnel. Sequential images of its top surface were measured during the same run to evaluate the effects of temperature change on PSP measurement. The pressure field obtained using an a-priori calibration method and a single-point measurement of model temperature was compared with the pressure tap measurements. In addition, Temperature-Sensitive Paint (TSP) was applied to measure the temperature distribution over the model in order to justify the correction method employed in this study. Finally the flow structures over the Ahmed model will be discussed by comparing PSP images with oil flow visualizations.

2. Sensors

2.1 Pressure-Sensitive Paint

PSP is a coating-type sensor that consists of luminescent molecules and a polymer binder. The sensor molecules in PSP are excited electronically to an elevated energy state, when illuminated with light at an appropriate wavelength. The excited molecules return to the ground state through several photochemical mechanisms; radiative decay (luminescence), non radiative decay (release of heat) and oxygen quenching. The principle of PSP is based on oxygen quenching. In the presence of oxygen molecules, the excited energy of sensor molecules is transferred to oxygen molecules, so that no luminescence is emitted. As a result, the luminescence intensity is reduced with increasing oxygen concentration or, in other words, oxygen partial pressure that is proportional to air pressure.

Theoretically, the relationship of the luminescence intensity I and the pressure P is expressed by the following relation, known as the Stern-Volmer relation:

$$\frac{I(P_{ref},T)}{I(P,T)} = A(T) + B(T)\frac{P}{P_{ref}} \tag{1}$$

where the subscript ref represents the reference conditions, and $A(T)$ and $B(T)$ are calibration coefficients. Note that these coefficients are functions of temperature T. Using Eq. (1), the surface pressure P can be calculated from the ratio of luminescence intensity images between the wind-on and wind-off (reference) conditions.

In actual practice, however, the temperature at the wind-on condition (T) is different from that at the wind-off condition (T_{ref}). Since PSP is dependant not only on pressure but also on temperature, it is necessary to carry out temperature correction to calculate the surface pressure. In such cases, Eq. (1) can be transformed into the following expression.

$$\frac{I(P_{ref},T_{ref})}{I(P,T)} = \alpha(T)\cdot\left(A(T) + B(T)\frac{P}{P_{ref}}\right) \tag{2}$$

where $\alpha(T) = I(P_{ref}, T_{ref})/I(P_{ref}, T)$. The factor $\alpha(T)$ is called the temperature correction factor.

In the present study, BF405 supplied by Innovative Scientific Solutions, Inc., is used as PSP. This paint emits phosphorescence with a peak wavelength of 650 nm, when excited by 405 nm light. The results of calibration tests of BF405 are shown in Fig. 1. It can be seen that the coefficients A and B of BF405 are independent of temperature. This is the characteristic known as “ideality” of PSP (Bell, 2004; Gouterman et al., 2004). Therefore, for BF405 paint, only the effect of temperature on α in Eq. (2) should be taken into account. In the following sections, the case for $\alpha = 1$ is termed ‘without temperature correction,’ while the case, where α is calculated using a single-point measurement of

model surface temperature, is termed 'with temperature correction.'

2.2 Temperature-Sensitive Paint

TSP is a sensor coating that consists of sensor molecules and a polymer binder. In contrast to PSP, TSP uses sensor molecules showing no oxygen quenching but having a relatively high activation energy for non-radiative decay. The luminescence intensity of TSP changes according to the Arrhenius equation and decreases with increasing temperature. For practical purposes, the paint characteristics can be expressed by the following polynomial equation:

$$\frac{I(T)}{I(T_{ref})} = \sum_{i=0}^{2} a_i \left(\frac{T}{T_{ref}} \right)^i \tag{3}$$

where a_i are the coefficient determined by calibration test.

The formulation of TSP used in the present work is as follows;

- Luminophore: Dichlorotris (1,10-phenanthroline)-ruthenium(Ⅱ) hydrate ($Ru(phen)^{+3}$)
- Binder: Polyacrylic Acid
- Solvent: Ethanol

The characteristic of Ru(phen)-based TSP is shown in Fig. 2 (Ohmi et al., 2006).

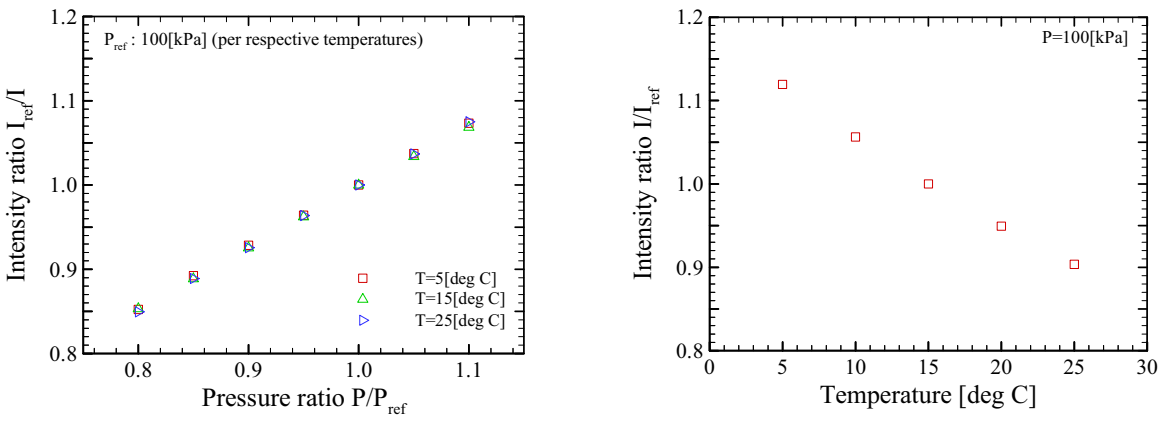

Fig. 1. Pressure and temperature sensitivities of BF405.

3. Experimental Setup

3.1 Model

The model used in this study was a 1/10 scale Ahmed model (Ahmed et al., 1984). A sketch of the model is shown in Fig. 3 (length: L = 104.4 mm, width: D = 38.9 mm, height: H = 28.8 mm). The model was made of aluminum alloy, and had a hollow structure. Eight pressure taps were provided along the center line of the model to compare with PSP results, and one thermocouple was mounted on the inner surface of the model to measure model substrate temperature. PSP and TSP were applied using an ordinary airbrush over a white base coat (T-6 041, Musashi Holt®) applied beforehand. Ten black dots (markers) were put on the top surface of the model for image registration.

3.2 Wind Tunnel

Experiments were conducted in the closed-circuit low-speed wind tunnel at the Institute of Fluid Science, Tohoku University. In the present experiment, an open-type test section with an octagonal

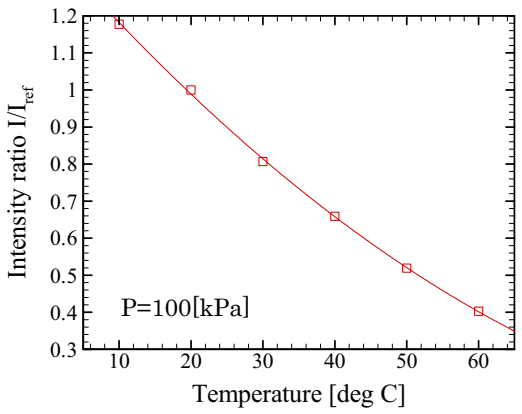

Fig. 2. Temperature sensitivity of Ru(phen)-based TSP.

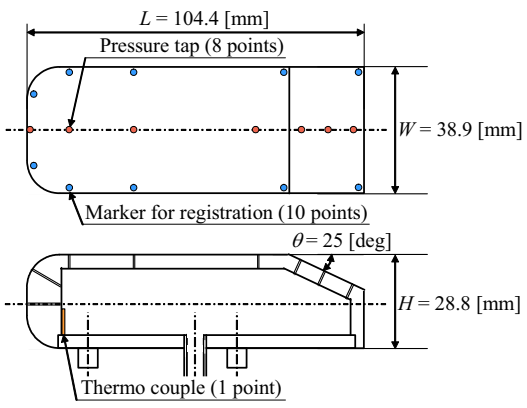

Fig. 3. Sketch of 1/10 scale Ahmed model.

cross section was used. The width of the test section was 293 mm and the length of test section was 940 mm. The model was installed on a flat plate (length: 600 mm, width: 296 mm, thickness: 15 mm) representing the ground plane. A rotary table was used to change the model yaw angle ϕ from 0 to 20 degrees. The freestream velocity was set at 50 m/s. The turbulence level of streamwise velocity was below 0.3 %. The Reynolds number *Re*, with respect to the length of the model *L*, was 3×10^5. The flow temperature was measured in the settling chamber of the tunnel using a resistance thermometer bulb. The typical temperature rise during a test was about 10 degrees Celsius.

3.3 Optical Measurement System

A schematic and a picture of the optical setup are shown in Fig.4. For PSP measurement, the excitation light source was two UV-LED units of which the peak wavelength was 395 nm. A band-passed filter (λ = 400±50 nm) was placed in front of the illumination unit in order to cut undesirable infrared emission from UV-LEDs. For TSP measurement, the excitation light source was a blue LED of which the peak wavelength is 470 nm. No filter was installed for the blue LED.

A luminescent intensity image was acquired using a 16-bit cooled CCD camera (HAMAMATSU, C4742-98). The spatial resolution was 1024 × 1024 pixels. Either a band-passed filter (λ = 650±20 nm) or a high-pass filter (λ > 580 nm) was placed in front of the camera lens for PSP and TSP measurements respectively to cut the excitation lights from LEDs.

3.4 Image Acquisition and Processing

In this study, PSP and TSP measurements were made only on the top surface of the model. The yaw angle was set either at ϕ = 0 or 20 deg. In both cases, several image sets were acquired during the run in the following sequence. Before starting the wind tunnel, a set of wind-off images '$I_{ref,\mathrm{before}}$' was acquired. After starting the wind tunnel, several sets of wind-on images, which were designated 'I_0', 'I_{10}' and 'I_{20}', were acquired at 10-minute intervals. Finally immediately after the tunnel was shut down, a set of wind-off images '$I_{ref,\mathrm{after}}$' was acquired. Each image set comprised 64 images. It took about 5 minutes to acquire one image data set. In calculating the ratio between the wind-off condition and the wind-on condition, the six combinations shown in Table 1 were evaluated. ΔT in Table 1 indicates the temperature difference between the wind-on and wind-off conditions. Here the temperature difference ΔT was calculated using the model substrate temperature measured by a thermocouple mounted on the inner surface of the model.

For TSP measurement, the obtained image data sets were designated as '$I_{T,ref,\mathrm{before}}$', '$I_{T,0}$', '$I_{T,10}$', '$I_{T,20}$' and '$I_{T,ref,\mathrm{after}}$' in the same way as PSP measurement. In calculating the temperature from TSP data, it was assumed that the temperature over the model was sufficiently uniform before the wind tunnel was started.

The PSP and TSP images were processed through a sequence of the following steps:

- Subtraction of dark images

- Ensemble averaging of 64 images
- Registration of the wind-on and wind-off images
- Calculation of luminescence intensity ratio
- Calculation of pressure and temperature using a-priori method

Correction of temperature by multiplying the temperature correction factor α, calculated from temperature measured by a thermocouple (in the case of PSP only).

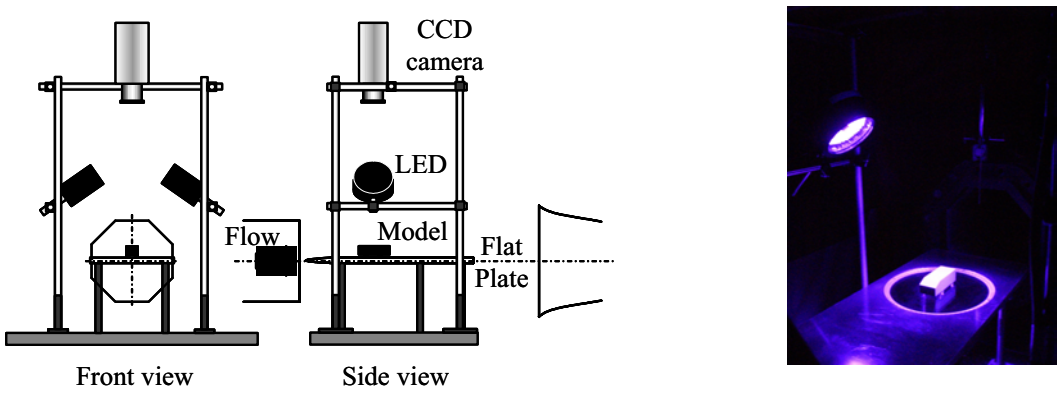

Fig. 4. Experimental setup.

Table 1. Combinations of wind-on and wind-off image sets.

Designation	Wind-off image	Wind-on image	ΔT [deg C]
Case1	$I_{ref,\,\mathrm{before}}$	I_0	2.9
Case2		I_{10}	7.1
Case3		I_{20}	9.0
Case4	$I_{ref,\mathrm{after}}$	I_0	6.2
Case5		I_{10}	2.0
Case6		I_{20}	0.1

4. Results and Discussions

4.1 Evaluation and Temperature Correction Method

The pressure profiles along the center line of the model are shown in Fig. 5 and Fig. 6 for six different combinations of the wind-off and wind-on images (Table 1). Figure 5 is the results for without temperature correction ($\alpha = 1$) and Fig. 6 for with temperature correction. It can be seen in Fig. 5 that temperature has a considerable effect on calculated pressure distribution (particularly in the absolute value). On the other hand, it can be seen in Fig. 6 that PSP data with temperature correction are in fairly good agreement with pressure tap data, compared to those without temperature correction. This agreement indicates that the proposed correction method using a single-point temperature measurement is effective, although it is not perfect. When the profiles in Fig. 6 are compared more carefully, it can be noticed that the shape of each profile is slightly different. In Region A (upstream), surface pressure at the immediate downstream of a suction peak, is flattened for cases 1 to 3, where $I_{ref,\mathrm{before}}$ is used as the wind-off image, but are decreasing for cases 4 to 6, where $I_{ref,\mathrm{after}}$ is used as the wind-off image. Also, in Region B (middle), the pressure profile is different in each case. For cases 4 to 6, the pressure distribution is more uniform than that for cases 1 to 3. It can also be noted that, in Region C (downstream), the pressure profile near the trailing edge is leveling off for cases 1 to 3, but is increasing for cases 4 to 6 (more realistic). It seems that these differences in pressure distribution are caused by the effect of local temperature distribution.

Figure 7 (images) and Fig. 8 (profiles) show surface temperature distribution on the model as measured by TSP. It can be seen that the model surface temperature increases monotonically with time during the test and varies in accordance with the flow pattern around the model. The high

temperature region at the front part of the model is considered to correspond to the region with the separation bubble. Spohn et al. (2002) showed that the vortex structure in the separation region is strongly unsteady, increasing the heat transfer rate and surface temperature. Likewise, the high temperature regions along the edges of the top surface correspond to the regions with high sharing forces.

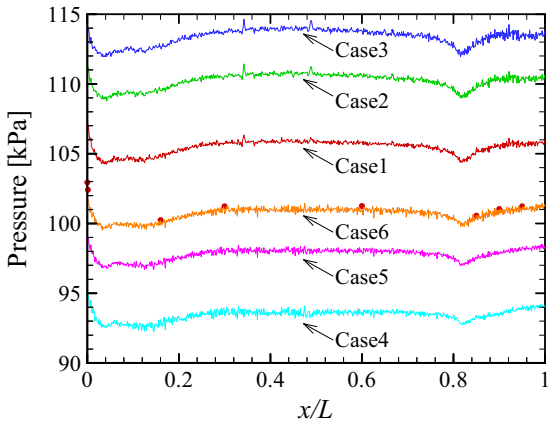

Fig. 5. Pressure profiles without temperature correction (—: PSP data for each cases, ●: Pressure tap data).

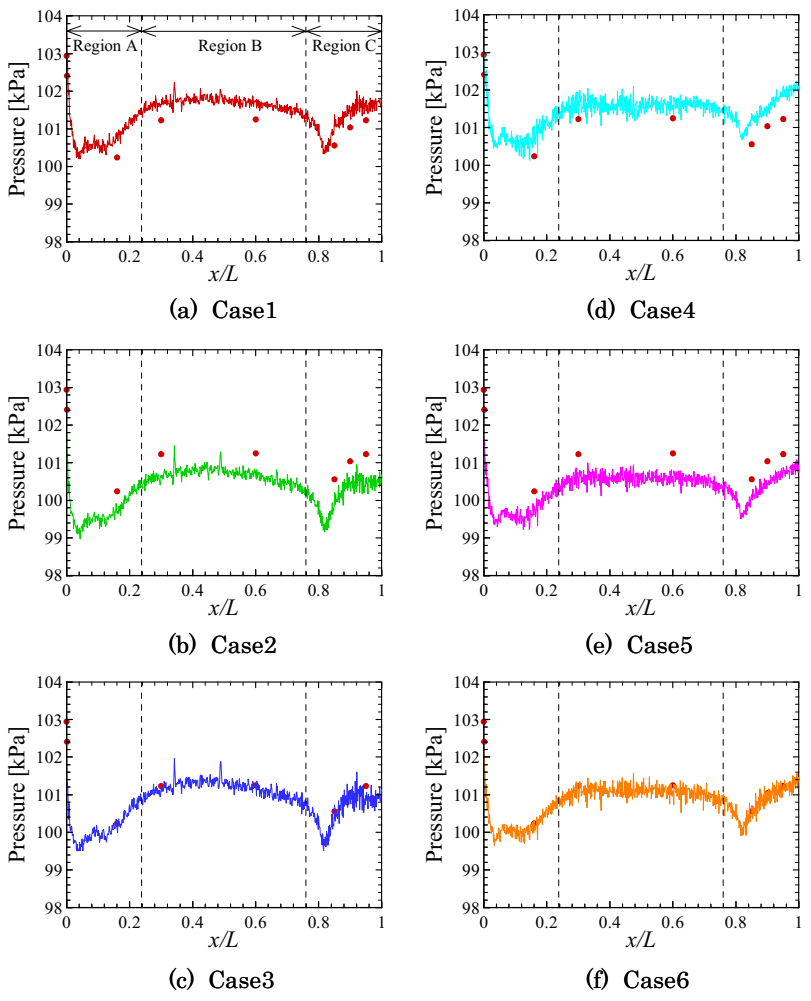

Fig. 6. Pressure profiles with temperature correction (—: PSP data for each cases, ●: Pressure tap data).

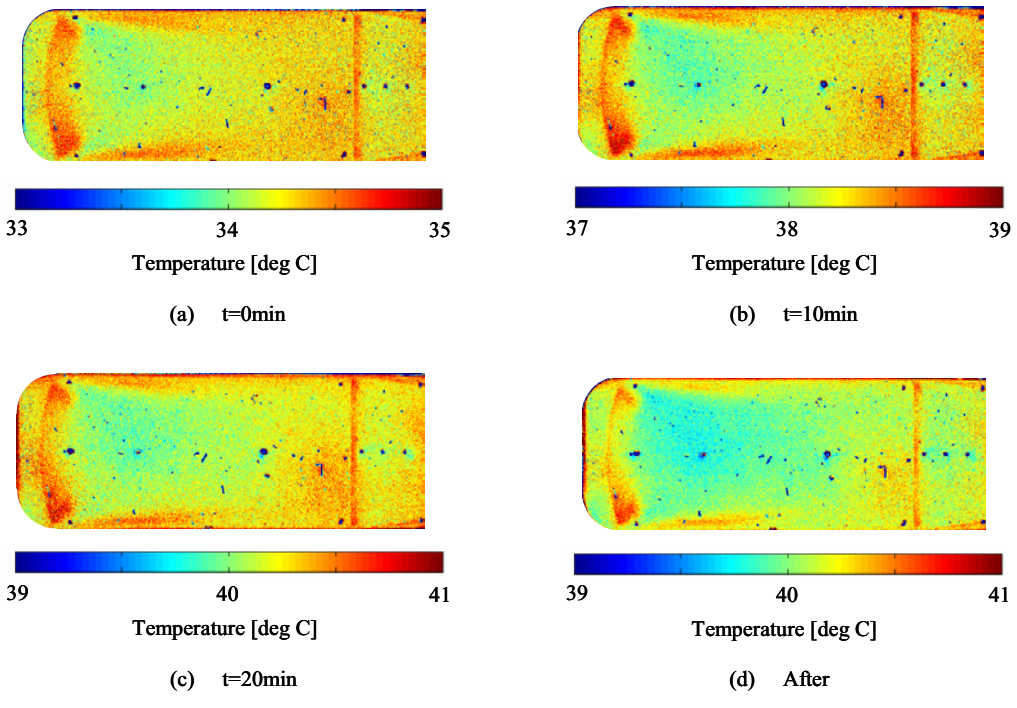

Fig. 7. Temperature distribution over the model in time.

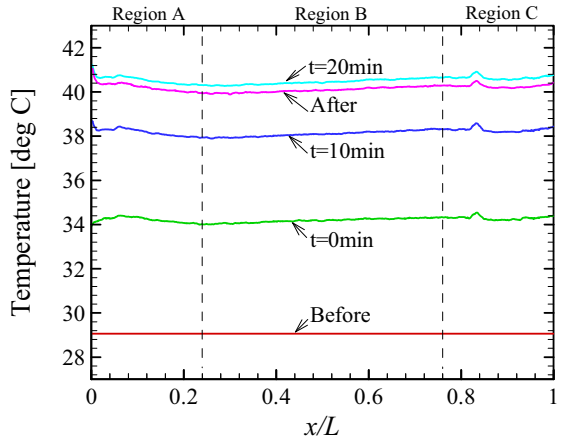

Fig. 8. Temperature profiles along the center line of the model.

Figure 9 compares the distribution of the temperature correction factor α along the center line of the model during the test time. It can be seen that the temperature correction factor α is constant over the model for Case 6, but not for the other cases. Additionally, the distribution of the temperature correction factor α over the top surface of the model for Case 6 is shown in Fig. 10. These figures show that temperature correction factor α is uniform over the model top surface. This means that the temperature correction method using a single-point temperature sensor can be justified only for Case 6. This is consistent with the experiences reported in the previous studies (Bell, 2004; Brown, 2000; Sant et al., 2001).

4.2 Analysis of Flow over the Ahmed Model

Pressure field images and corresponding oil flow visualization are shown in Fig. 11 and Fig. 12, respectively, for the cases of the yaw angle $\phi = 0$ and 20 deg. It can be seen that PSP images capture the complex flow structure over the Ahmed model.

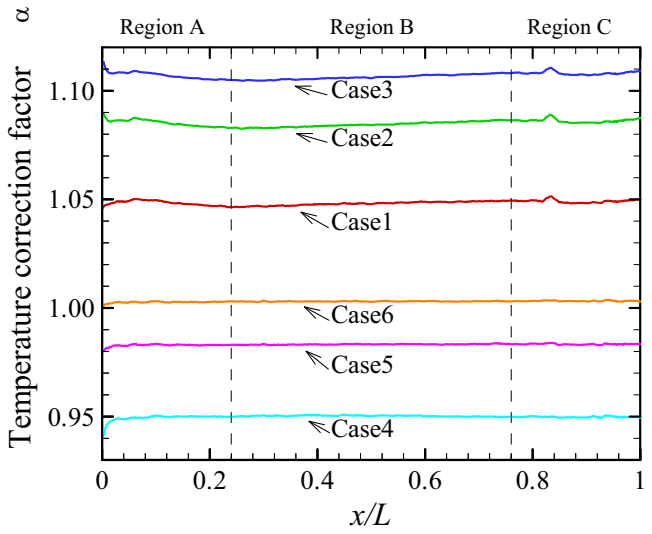

Fig. 9. Profiles of temperature correction factor along the center line of the model.

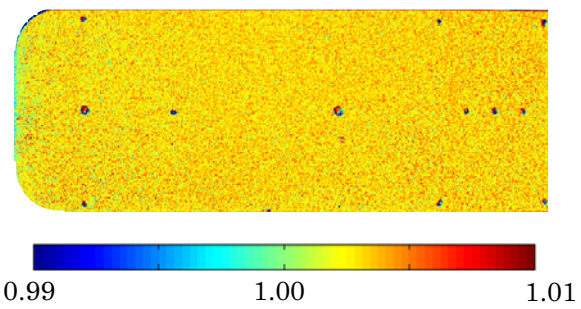

Fig. 10. Distribution of temperature correction factor for Case 6.

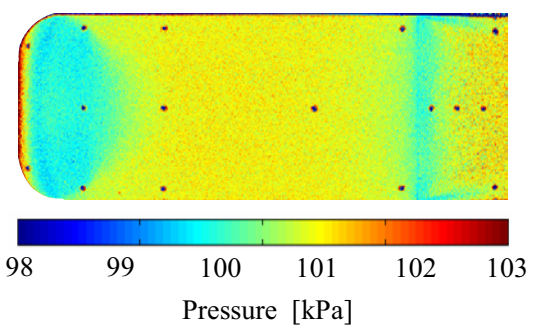

(a) PSP

(b) Oil Flow

Fig. 11. Visualization in the case of $\phi = 0$ [deg].

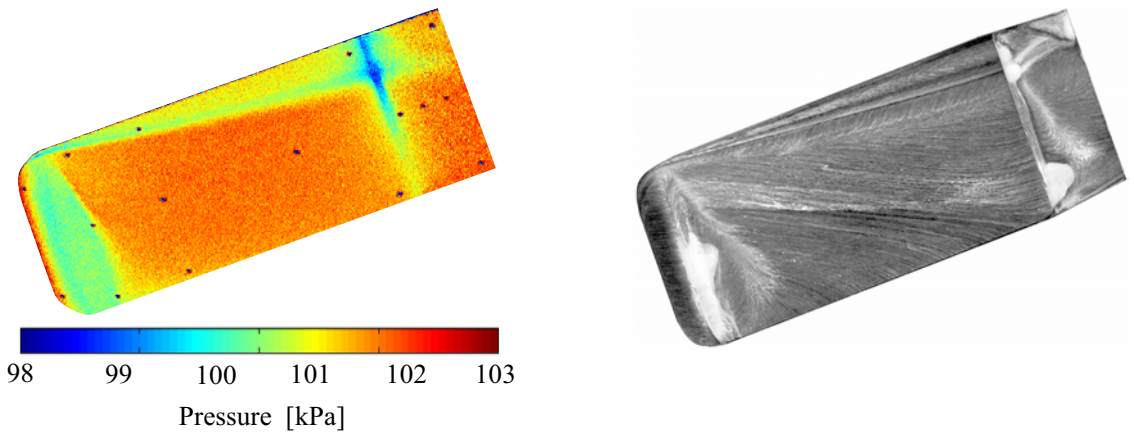

(a) PSP (b) Oil Flow

Fig. 12. Visualization in the case of ϕ = 20 [deg].

In the case of ϕ = 0 deg, a suction peak and a separation bubble are visualized near the front part of the model. On the other hand, counter rotating cone-like trailing edge vortices can be seen along the two side edges of the slant surface. The existence of such vortex structures on the slant has also been reported in previous studies (Spohn et al., 2002; Krajnovic et al., 2004).

In the case of ϕ = 20 deg, a complex vortex structure, similar to the leading edge separation of a delta wing, can be seen on the right-hand side of the model. Similar to the case of ϕ = 0 deg, the low pressure region at the front part of the model is caused by flow separation that is open at the left-hand side of the model, suggesting a vortex is shed downstream from this point. The flow field near the intersection between the roof and the slant is more complicated due to vortex-vortex interaction. The negative pressure region at the front edge of the slant is probably caused by a strong vortex, but the detailed flow structure is not clear in the oil flow. It would be necessary to combine PSP and other visualization techniques like PIV or laser light sheet to understand the flow field on the slant in more detail.

5. Conclusions

The effects of surface temperature on PSP measurement were investigated in an attempt to develop a correction method for temperature in low-speed tests. An experiment was conducted using a simplified car model known as the Ahmed model and PSP and TSP images on the model top surface were acquired over the entire test period including the cases before and after the run. The conclusions drawn from this experiment can be summarized as follows;

1. The errors caused by model temperature distribution can be reduced using the temperature correction factor (α) calculated from a single-point measurement of model temperature.
2. From the results of TSP tests, it has been justified that the most accurate result is obtained by using the wind-off image acquired immediately after the tunnel is shut down and the wind-on image acquired immediately before the tunnel is shut down.
3. Using the present measurement technique, the complex pressure fields over the Ahmed model, caused by flow separation, reattachment and vortices, were successfully visualized.

References

Ahmed, S. R., Ramm, R. and Faltin, G., Some salient features of the time-averaged ground vehicle wake, SAE Paper 840300 (1984).

Bell, J. H., Schairer, E. T., Hand, L.A. and Mehta, R.D., Surface Pressure Measurements Using Luminescence Coatings, Ann. Rev. Fluid Mech., 33 (2001), 155-206.

Bell, J. H., Application of Pressure-Sensitive Paint to Testing at Very Low Flow Speeds, 42nd AIAA Aerospace Sciences Meeting and Exhibit (Reno, Nevada), AIAA 2004-0878 (2004).
Brown, O., Low-Speed Pressure Measurements Using a Luminescent Coating System, (2000), Ph.D Thesis, Stanford University.
Engler, R. H., Merienne, M. C., Klein, C. and Sant, Y. L., Application of PSP in low speed flows, Aerospace Science and Technology, 6 (2002), 313-322.
Gouterman, M., Callis, J., Dalton, L., Khalil, G., Mebarki, Y., Cooper, K. R. and Grenier, M., Dual luminophore pressure-sensitive paint: Ⅲ. Application to automotive model testing, Meas. Sci. Technol., 15 (2004), 1986-1994.
Krajnovic, S. and Davidson, L., Large-Eddy Simulation of the Flow Around Simplified Car Model, 2004 SAE World Congress (Detroit), SAE Paper 2004-01-0227 (2004).
Mebarki, Y. and Cooper, K. R., Aerodynamic Testing of a Generic Automotive Model with Pressure Sensitive Paint, 10th International Symposium on Flow Visualization (Kyoto, JAPAN), ISFV-20020F0120 (2002).
Mitsuo, K., Kurita, M., Nakakita, K. and Watanabe, S., Temperature Correction of PSP Measurement for Low-Speed Flow Using Infrared Camera, 21st International Congress on Instrumentation in Aerospace Simulation Facilities (Sendai, JAPAN), 10-1 (2005).
Ohmi, S., Nagai, H., Asai, K. and Nakakita, K., Effect of TSP Layer Thickness on Grobal Heat Transfer Measurement in Hypersonic Flow, 44th AIAA Aerospace Sciences Meeting and Exhibit (Reno, Nevada), AIAA 2006-1048 (2006).
Sant, Y. L., Bouvier, F., Merienne, M. C. and Peron, J. L., Low Speed Tests using PSP at ONERA, 39th AIAA Aerospace Sciences Meeting and Exhibit (Reno, Nevada), AIAA 2001-0555 (2001).
Spohn, A. and Gillieron, P., Flow Separations Generated by a Simplified Geometry of an Automobile Vehicle, IUTAM Symposium on Unsteady Separated Flows (Toulouse, France), (2002).

Author Profile

Taro Yamashita: He received his B.S. and M.S. degrees in Aerospace Engineering from Tohoku University in 2003 and 2005 respectively, where he studied the wake behind bluff bodies and the development of a Magnetic Suspension and Balance System. Now he is studying on a Ph.D. course at Tohoku University. His current research topic is the application of molecular sensors to low-speed flow.

Hikaru Sugiura: He received a B.S. degree in Mechanical Engineering from Tokyo Metropolitan University in 2005. And he received a M.S. degree in Aerospace Engineering from Tohoku University in 2007. Now he has been working for IHI Co., Ltd. since 2007.

Hiroki Nagai: He received his Ph.D. degrees in Institute of Engineering Mechanics and Systems from University of Tsukuba in 2000 for a study of shock waves in superfluid helium. He worked from 2001 to 2003 with National Space Development Agency of Japan (Predecessor: Japan Aerospace Exploration Agency (JAXA)) as a researcher, where he engaged in the development of thermal control device and thermal analysis of spacecraft. Since 2003, he worked as a Research Associate at Aerospace Engineering of Tohoku University. His current research topics are to apply PSP measurements in micro devices such as micronozzle, microchannel, and microturbine, and to establish the flow diagnostic technique in micro-scale flow.

Keisuke Asai: He is a Professor of Aerospace Engineering at Tohoku University. He graduated from Kyoto University 1980 and obtained his PhD in Aeronautics and Astronautics from Tokyo University in 1995. He worked for National Aerospace Laboratory (NAL) from 1980 to 2003, before moving to Tohoku University. From 1999 to 2003, he promoted “MOSAIC” that is an interdisciplinary research project to develop molecular sensor technology. His research interests involve development of molecular sensor technology for extreme flow conditions and its applications to cryogenic wind tunnels, hypersonic wind tunnels, and micro-scale gas flows. He is member of AIAA AMT-TC and ICIASF-Panel.

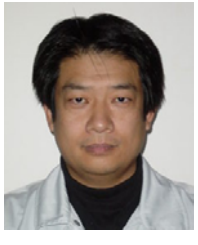

Keitaro Ishida: He has been working for Nissan Motor Co. Ltd. since 1990. Now he belongs to the Measuring Engineering Department. His current work includes developing hydropneumatic measurement, calibration for hydropneumatic measuring instruments, and the development of sensor technology for measurement and flow visualization.